Rapidity and Transverse Momentum of D mesons from $D^{\pm}_{(S)} \to \phi\pi^{\pm} \to K^{+}K^{-}\pi^{\pm}$ Decay

Ellen Holmgren

Advisor: Professor Robert Harr

Wayne State University

August 12, 2016

Abstract

The goal of this project is to measure the $D^{\pm}_{(S)}$ rapidity and transverse momentum in CDF Run 2 data. While previous studies have done similar analyses for transverse momenta between 4-20 GeV/c [1] , we have more data and a higher momentum range from 4 - 70 GeV/c. Through more bins and higher momentum, we hope to create a more thorough picture of $D^{\pm}_{(S)}$ momentum and rapidity distributions.

1 Background

1.1 Particle Physics

The goal of the field of particle physics is to test and further the understanding of the standard model of particle physics. The standard model theory classifies fundamental particles that make up matter: quarks, and leptons. It also classifies the particles behind the forces that bind them together, gauge bosons [2]. These particles are displayed in Fig. 1. This project focuses on a type of hadron called a meson, which is formed from a quark and antiquark. Specifically it focuses on the charm mesons, D^+ which is $c\bar{d}$, and D_S^+ which is $c\bar{s}$ and their charge conjugates. This analysis measures the rapidity distribution and momentum distribution of these mesons after a $p\bar{p}$ (proton and antiproton) collision. Moreover, it investigates how these distributions are related or not related. Understanding D^+ and D_S^+ rapidity and momentum allows physicists to predict what direction and with what momentum these mesons are likely to be produced.

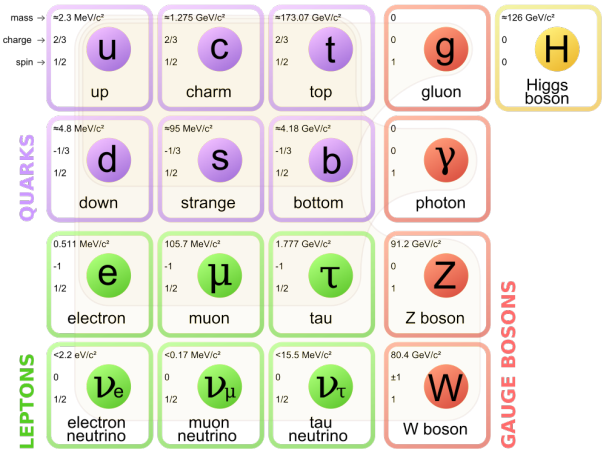

Figure 1: The Standard Model of Elementary Particles in Particle Physics [3].

1.2 Overview of D^+ and D_S^+ Decay and Detection

After a $p\bar{p}$ collision, the D^+ and D_S^+ created are not stable. They quickly decay into other mesons:

$$D_{(S)}^{\pm} \to \phi\pi^{\pm} \to K^+K^-\pi^{\pm} \tag{1}$$

It follows, that to study the D mesons the particle detectors detect the kaon pair and pion and use their characteristics to reconstruct the decay and determine the original D meson's characteristics. Of course, the pion and kaon pair still have to be detected through their interactions with other matter. In the CDF detector, these mesons leave a trail of hits, which are observed interactions. These hits are analyzed to determine a track, this is a sequence of hits that is most likely from a single particle. Then the track is analyzed to identify traits about that particle.

1.3 CDF Detector

Each track is created as the particle traveled through two detection chambers, the silicon detector chamber and central outer tracker (COT). Both chambers are inside a solenoid which creates a magnetic field. Immediately beyond the $p\bar{p}$ collision beam line, charged particles encounter the silicon detector, which is in peach on Fig. 2 and below the COT in Fig. 3. This compact detector was composed of seven concentric rings which recorded charge, location, and direction. Next the larger Central Outer Tracker continued to record hits. The COT is the tan chamber in Fig. 2 and clearly labeled in Fig. 3.

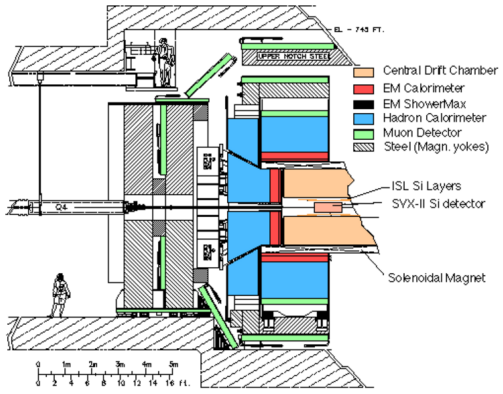

Figure 2: Cross Section of CDF Detector [4]

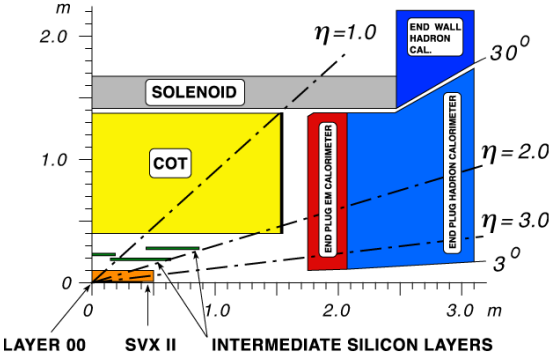

Figure 3: CDF Detector Geometry with some Pseudorapidity Measurements [5]

Together, these detection chambers measure the particle's charge, pseudorapidity, reconstructed path, impact parameter and momentum. The direction the particle curves in the magnetic field is determined by it's charge. The pseudorapidity is a measurement of the angle from the proton beam line as shown in Fig. 3. It is defined by the formula $\eta = -\ln\left[\tan\left(\frac{\theta}{2}\right)\right]$. Later, the rapidity is defined by $y = \frac{1}{2}\ln\left(\frac{E+\rho_z c}{E-\rho_z c}\right)$. The pseudorapidity allows the particle's full path to be reconstructed with other information about its direction of travel. This means a pair of kaons can be traced back to where they decayed from a phi meson and the phi meson can be traced back to where it decayed from a D^+. The distance between the appearance of a particle and the original event is called its decay length. The overall radius of the curve is used to deduce the particle transverse momentum. [6]

1.4 CDF Triggers

Of course this is only a description of a single particle's movement but there are 3 million possible events to detect every second after a $p\bar{p}$ collision. Hence, an automated system was created with three levels of triggers to make informed selections as the pieces data are processed. This means

that not all possible decays are saved. The data analyzed here are selected by a two track trigger which means, the trigger is analyzing two tracks that could have originated from the same decay. Since, this project is focused on transverse momentum it was directly affected by the cuts in Table 1. As a result, all fitting and results were separated by trigger.

	Loosest Trigger	Medium Trigger	Tightest Trigger
Each Particle's Momentum	> 2 GeV/c	> 2 GeV/c	> 2.5 GeV/c
Sum of Momentum	> 4 GeV/c	> 5.5 GeV/c	> 6.5 GeV/c
Particles Oppositely Charged	No	Yes	Yes

Table 1: Examples of Cuts for Different Triggers

1.5 CDF Simulation

As well as recording data from real events, CDF uses a Monte Carlo simulation to simulate data sets based on known parameters. In part this simulation goes toward helping to achieve an efficiency calculation. This calculation is an estimate of the fraction retained by the trigger selection and fitting of the data.

1.6 Data Processing

Once a set of data was simulated or recorded, it had to be processed as shown below in Figure 4.

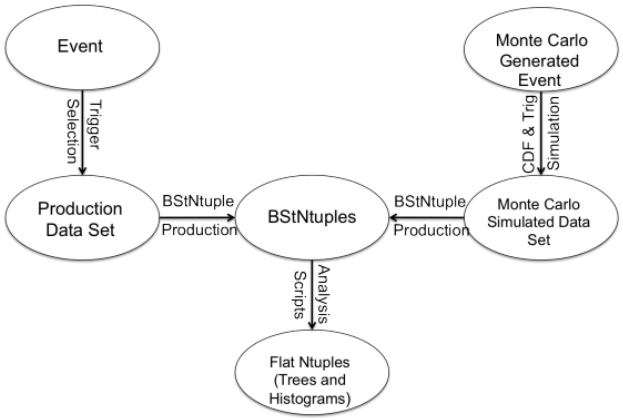

Figure 4: The flow of data [7].

2 Procedure

The work began with the data from the CDF experiment already organized into flat ntuples (histograms and trees). The first step was to organize the data from the flat ntuple through

binning and creating histograms with the bins. We binned in KK mass, trigger bit, transverse momentum and rapidity. The intention in binning was to create relatively equal numbers of events in each bin with enough events to be fit well but few enough bins so that we could see the behavior of the particle (and so that the behavior could be fit to a curve). Some of the different binnings we tried are listed in Table 2 with their advantages and disadvantages. We decided to use five rapidity bins so that changes in momentum behavior with different rapidity would be clear. As a result, in each momentum binning we had some error in the lower and higher bins. Since the momentum decreased exponentially there were not many events in the last bin. The trigger selection process also affected the number of events in lower momentum bins. Once the data were binned, each bin was used to create a two dimensional histogram of KK mass vs impact parameter as shown in Fig. 5.

Table 2: Different Momentum Binning and the Advantages and Disadvantages

	Binning 1	Binning 2
Total Number of Bins	8	9
Bin 1 (GeV/c)	4-6	4-5.5
Bin 2 (GeV/c)	6-7	5.5-6.5
Last Bin (GeV/c)	16-70	20-70
Advantages	Fewer empty bins	Bin Edges at Trigger pt cuts
Disadvantages	Behavior less clear	More empty or almost empty Bins

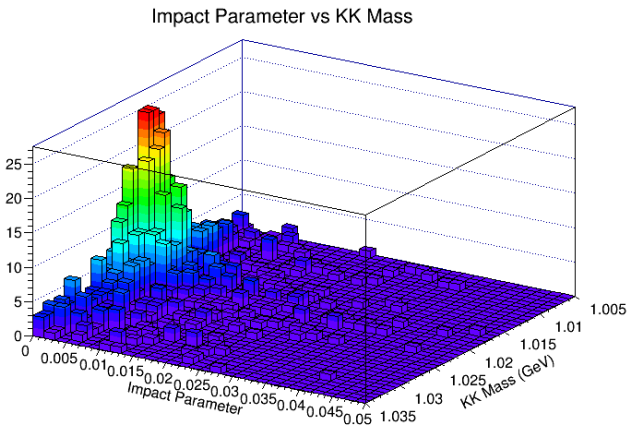

Figure 5: Impact Parameter vs KK Mass Before Fitting for a Sample Bin

As shown in Fig. 6 and Fig. 7 we used fitting scripts to select prompt signal events and disregard non-prompt signal, prompt background and non-prompt background. Fig. 6 and Fig. 7 show the process for the bin from Fig. 5 but each bin underwent the same fitting process. We used impact parameter to model prompt and non-prompt events. Prompt events are defined as decays that decayed directly from the $p\bar{p}$ collision. Meanwhile, non-prompt events are decays from D mesons that decayed from B mesons instead of directly from the $p\bar{p}$ collision. We modeled the prompt events with a Gaussian. Meanwhile, we modeled non-prompt events with

an exponential convolved with a Gaussian. The impact parameter axis is graphed in Fig. 6 for a single bin. Through KK mass fitting, we defined signal as events that fit a KK Mass curve and modeled this curve with a relativistic Briet-Wigner convolved with a Gaussian. Background was fit with an Argus function in order to remove events that were mostly likely not kaon pairs. The KK mass fitting is easiest to see from Fig. 7. In both Fig 6 and 7, the data along the blue model line was selected as prompt signal and was fit to D^+ and D_S^+ mass curves next.

Two Dimensional Fitting for an Example Bin: Impact Parameter and KK Mass

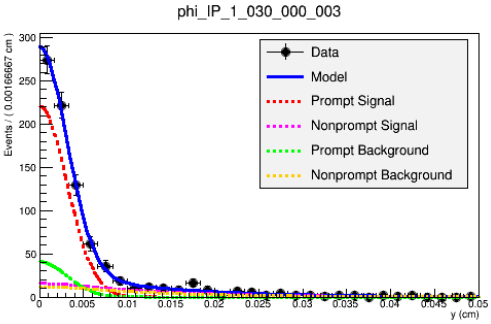

Figure 6: Impact Parameter fit

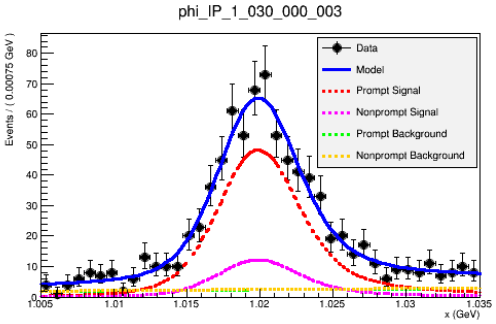

Figure 7: KK Mass Fit

For this step, each histogram went through a signal fit to select data that matched the signal curve for the $D^{\pm}$ and $D_S^{\pm}$ masses. Both $D^{\pm}$ and $D_S^{\pm}$ mesons had expected peaks fit by two Gaussian with the same mean but different widths. Meanwhile, the background was fit to an exponential decay, a square root function and a small Gaussian centered above 2 GeV and those events were filtered out. An example of these fits is shown in Fig. 8. At the end of this script we created a two dimensional histogram of rapidity vs momentum with just the events that had passed all of the fits. Although this histogram had an accurate shape, we had no way of knowing what fraction of D^+ and D_S^+ decay events we had selected. In other words, we needed to know the efficiency of the fits.

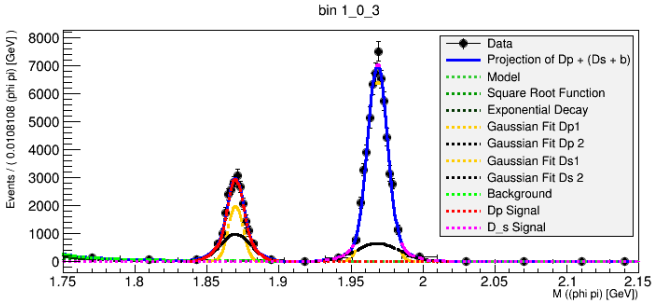

Figure 8: The D^+ and D_S^+ fits from the second fitting script.

To calculate the efficiency, we began working with Monte Carlo simulation data. We had about 10 million events simulated for both $D^{\pm}$ and $D_S^{\pm}$. We created two histograms from the

simulation, one was from the generated data before any fits and the second was from data that was run through the same fitting scripts as the real data. In order for the fits to work accurately, we created a simulation of background data from a small subsection of the real data so the simulation could mimic the data and the fitting scripts would not crash. Then we divided the reconstructed fit of the simulation by all of the generated to get the efficiency. Once the simulation had gone through the same process as the rest of the data, we calculated the efficiency histogram:

$$\text{Efficiency} = \frac{\text{Reconstructed, fitted Simulation}}{\text{Generated Level Simulation}} \tag{2}$$

and adjusted the data to reflect it:

$$\text{Adjusted data} = \frac{\text{Reconstructed Data}}{\text{Efficiency}} \tag{3}$$

At this point, we had the first set of preliminary results.

3 Preliminary Results

We have a set of data now that has gone through the correct process but hasn't had all of the checks it needs in order to be confirmed. In Addendum 1 after the Bibliography, we attached these graphs in bulk with their momentum cross sections by rapidity bin and with the two dimensional histogram side by side.

One check we have currently explored is bin smearing. Bin smearing refers to the fact that some of the events are reconstructed in different bins than they are generated in. We used the generated simulation to create a histogram for each momentum and rapidity bin by filling every bin of the histogram with that single target bin as shown in Fig. 9.

Transverse Momentum Bin 6 in Trigger 3: Bin Smearing

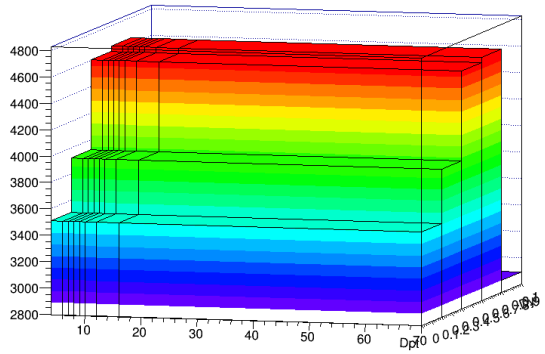

Figure 9: The Generated Level

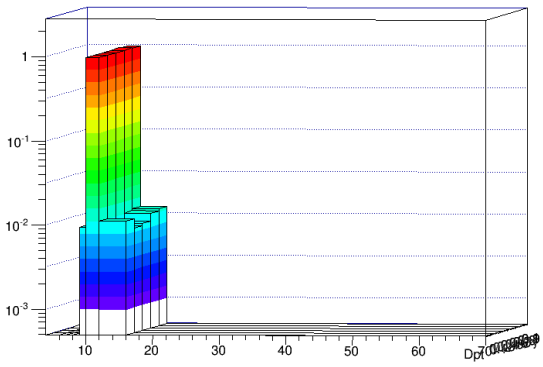

Figure 10: Fraction of Events in Generated Bin

Then we filled a histogram with reconstructed data from the events that were generated in

target bin. We divided this histogram by the generated simulation histogram (for momentum bin 6 see Fig. 9). The result is a histogram which shows the fraction of results that is reconstructed into the same bin. This is shown in Fig. 10. We looked at these results in text form to have a more quantitative understanding. In the momentum bins, 95% - 98% of the generated events were being reconstructed into the same bin. Meanwhile, the rapidity bins were closer to 97% -99 % of the generated events being reconstructed into the same bin. In further study this data check should be more thoroughly processed and taken into account in the error or corrected.

4 Further Study

Right now, there is far less simulated data than real so it is suspected that some of the fits are not functioning properly over bins with low numbers of simulated events. As a result, we are in the process of simulating a dataset that is ten times larger. Once that is complete, we can run it though the current set of scripts and move on to ruling out other error sources. For example, we need to explore track efficiency and quantify the error from bin smearing. Although work remains, we have made significant progress towards a reliable result. With this set of measurements, we have the information we need to make informed decisions in the final steps of this project and get a publishable result.

References

[1] D.Acosta *et al.* CDF II Collaboration. Measurement of prompt charm meson production cross sections in $p\bar{p}$ collisions at $\sqrt{s} = 1.96$ tev. *Physical Review Letters*, 91(24):1–7, 12 2003.

[2] Nari Mistry. A brief introduction to particle physics. *Cornell University, USA*, 2000.

[3] MissMJ on Wikipedia Commons. Standard model of elementary particles, 2006. [Online; accessed July 29, 2016].

[4] FermiLab. Elevation view of cdf, Unknown. [Online; accessed August 1, 2016].

[5] FermiLab. Silicon tracking system, Unknown. [Online; accessed August 1, 2016].

[6] Jennifer Lauren Lee. Cdf virtual tour, 2008.

[7] D Fitzgerald. A search for exclusive fully reconstructed w boson decays in cdf run ii data. page 8, 2015.

5 Addendum 1: Prelinary Results Graphs

5.1 D^+ Meson

D^+ Trigger 1; Loose

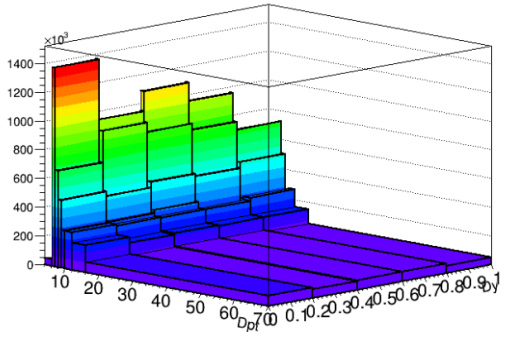

Figure 11: Two-Dimensional Histogram

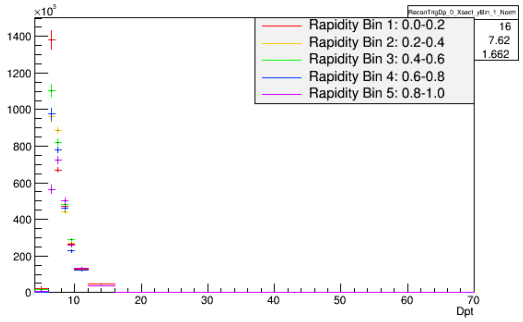

Figure 12: Transverse Momentum Cross Sections by Rapidity bin

D^+ Trigger 2; Medium

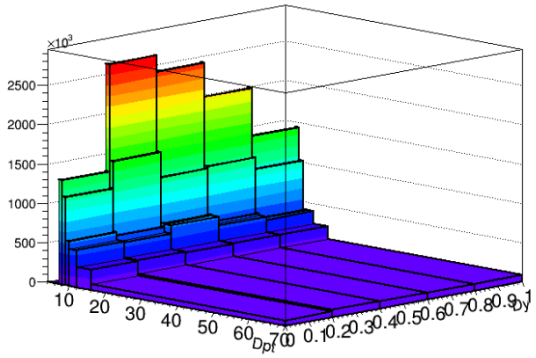

Figure 13: Two-Dimensional Histogram

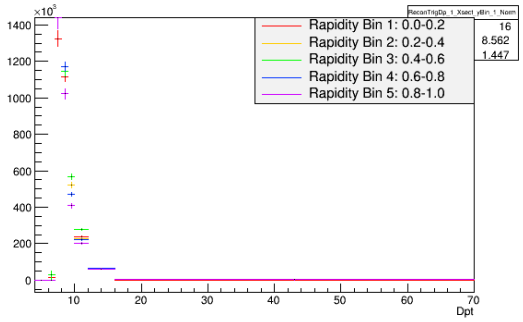

Figure 14: Transverse Momentum Cross Sections by Rapidity bin

D^+ Trigger 3; Tight

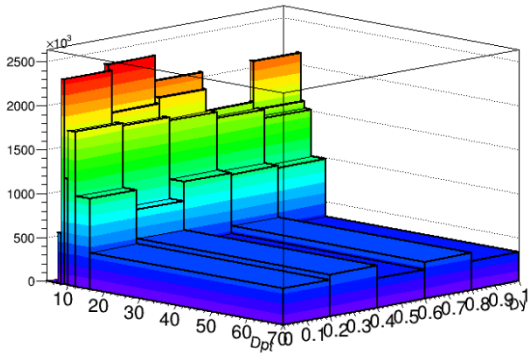

Figure 15: Two-Dimensional Histogram

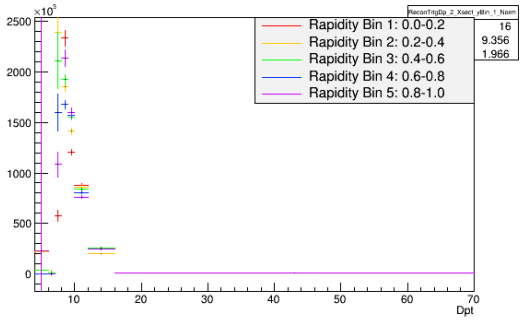

Figure 16: Transverse Momentum Cross Sections by Rapidity bin

Efficiencies

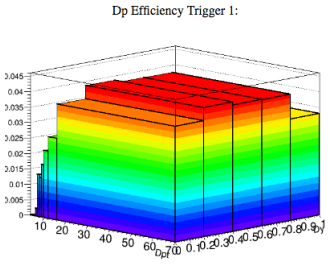

Figure 17: D^+ Trigger 1

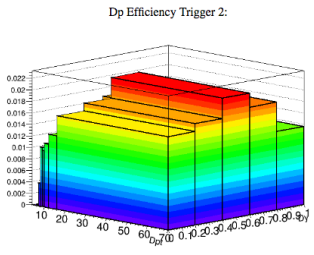

Figure 18: D^+ Trigger 2

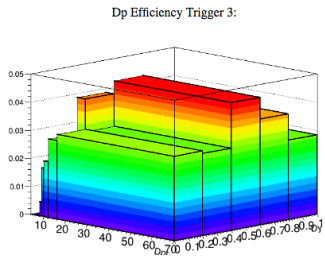

Figure 19: D^+ Trigger 3

5.2 D_S^+ Meson

D_S^+ Trigger 1; Loose

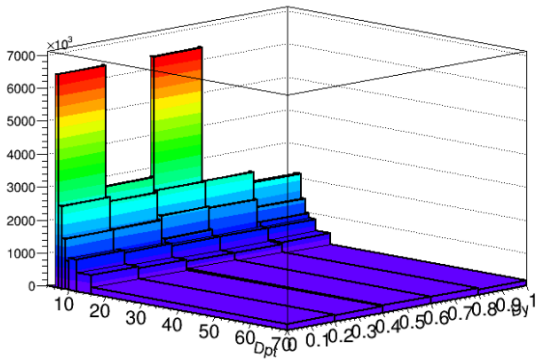

Figure 20: Two-Dimensional Histogram

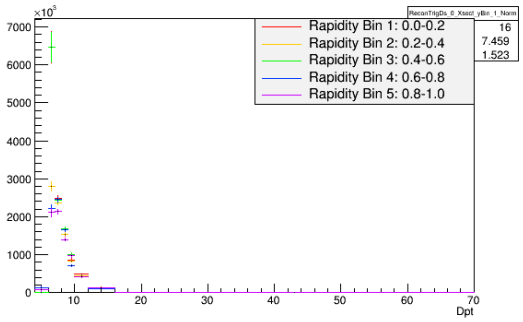

Figure 21: Transverse Momentum Cross Sections by Rapidity bin

D_S^+ Trigger 2; Medium

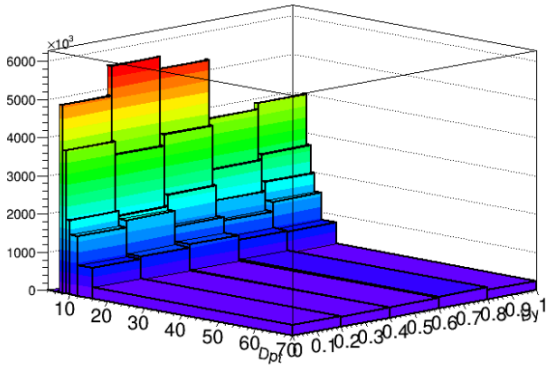

Figure 22: Two-Dimensional Histogram

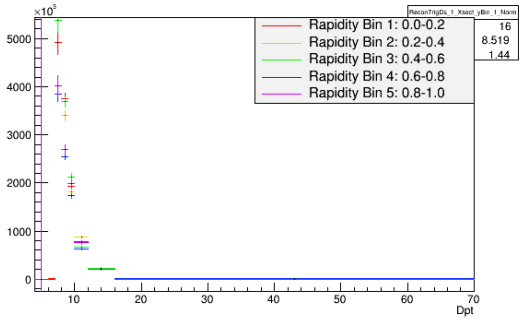

Figure 23: Transverse Momentum Cross Sections by Rapidity bin

D_S^+ Trigger 3; Tight

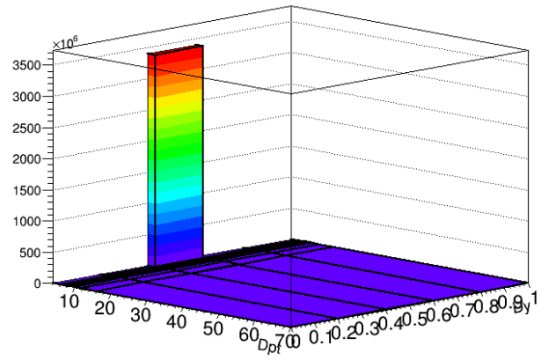

Figure 24: Two-Dimensional Histogram

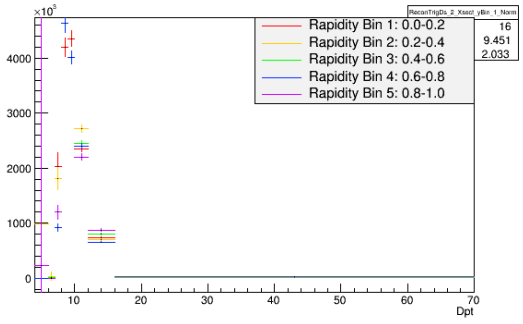

Figure 25: Transverse Momentum Cross Sections by Rapidity bin

Efficiencies:

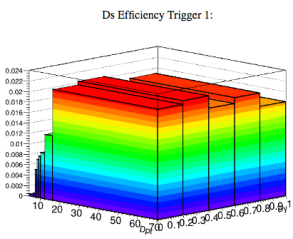

Figure 26: Ds Trigger 1

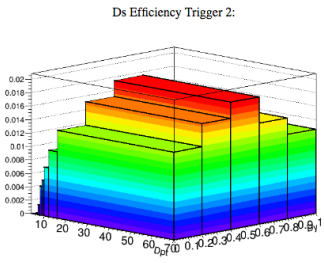

Figure 27: Ds Trigger 2

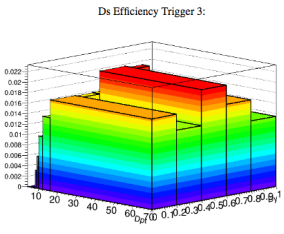

Figure 28: Ds Trigger 3